https://doi.org/10.48048/tis.2022.2685

MHD Mixed Convective Slip Flow along an Inclined Porous Plate in Presence of Viscous Dissipation and Thermal Radiation

Sharad Sinha[*] and Rajendra Singh Yadav

Department of Mathematics, University of Rajasthan, Jaipur 302004, India

([*]Corresponding author's e-mail: sharadsinha89@gmail.com)

Received: 30 March 2021, Revised: 23 June 2021, Accepted: 30 June 2021

Abstract

The present study investigates the mixed convective MHD flow of Newtonian fluid along an inclined permeable plate which is saturated in porous medium. A non-uniform magnetic field along with viscous dissipation and thermal radiation is also considered in the model. Velocity and thermal slip conditions are applied at the plate. Expressions for skin friction and Nusselt number are obtained with the help of suitable similarity transformation. Governing equations are solved numerically by Runge-Kutta fourth order method with shooting technique. Graphs of the fluid velocity and temperature are plotted and their behaviours are discussed. Numerical values of skin friction and Nusselt number are tabulated and analysed.

Keywords: MHD, Porous medium, Slip effect, Radiation, Viscous dissipation

Introduction

During past few years, study of mixed convection with viscous dissipation and thermal radiation of viscous incompressible MHD fluids have attracted attention because of its wide applications in astrophysics, geophysics, manufacturing industries, missile aerodynamics, heating room and buildings by use of radiators etc. Knowledge of porous media is important because of its vast use in filtration, hydrology, soil mechanics, petroleum geology and others.

MHD fluid flow has the property to control separation flow, optimizes the heat transfer and it was first introduced by Ferraro and Plumpton [1]. Jaluria [2] presented a detailed discussion on heat and mass transfer by natural convection. Later Afzal and Hussain [3] extended the idea of natural convection to mixed convection and investigated the effect on flow along a horizontal plate. Hossain and Takhar [4] considered the study of Afzal and Hussain [3] and analyzed the radiation effects on it with vertical plate of uniform surface temperature in all 3 modes of convection. Pop and Ingham [5] done a comprehensive study of different models of convective heat transfer in viscous fluids through porous medium. Damesh [6] took a vertical surface saturated in porous medium and discussed mixed convective flow along with external magnetic field and radiation effects, and obtained that increasing radiation parameter results in decreasing local Nusselt number. Aydin and Kaya [7] presented viscous dissipation effects in mixed convective flow along a vertical flat plate and discussed mixed convection flow situations depending upon aiding/opposing buoyancy and viscous dissipation. Later Cao and Baker [8] used first order interfacial velocity and thermal slip effects in mixed convective flow from a vertical plate and explained the flow and heat transfer numerically. Bhattacharyya *et al.* [9] discussed slip flow and heat transfer over a horizontal plate with external magnetic field. Nandeppanavar *et al.* [10] explained effects of thermal radiation and non-uniform heat source/sink on MHD flow and heat transfer by considering a model of extrusion process. In the presence of radiation and buoyancy effects, natural convection through permeable surface was investigated by Rashidi *et al.* [11]. Sharma and Choudhary [12] used perturbation technique and analyzed the inclined magnetic field and radiation effects on slip flow over a permeable plate. Later Das *et al.* [13] included Joule heating and viscous dissipation effects in their study to generalize the MHD mixed convective slip flow over a porous plate and shown that due to viscous dissipation and Joule heating shear stress and heat transfer decrease at the plate. Suction/injection and viscous dissipation effects on MHD slip flow through porous medium was analyzed by Pandey and Kumar [14]. Sharma *et al.* [15] investigated the influence of various physical parameters on MHD mixed convective flow along vertical surface with heat source and sink. Recently Krishna *et al.* [16] considered

exponential accelerated plate in porous medium and discussed MHD free convective rotating flow over it with chemical reaction. Sheikholeslami *et al.* [17] used multiple twisted tapes in a solar flat plate collector to analyze the entropy and thermal behaviour of Aluminium Oxide- water nanofluid. Later Sheikholeslami *et al.* [18,19] presented a detailed study to decrease the temperature of photovoltaic modules by various nanofluids. The study revealed that by using nanofluids energy efficiency of solar collectors can be enhanced.

In the present work our objective is to investigate the effects of viscous dissipation, thermal radiation and suction through permeable plate in the presence of heat source and heat sink respectively, on mixed convective MHD slip flow along an inclined plate.

Mathematical formulation

Steady 2 dimensional mixed convective laminar MHD boundary layer flow of viscous incompressible fluid along a permeable plate is considered. The plate is inclined with an angle γ from the vertical and saturated in a porous medium. x-axis is taken along the plate and y-axis is normal to it. Velocity components in x and y directions are u and v, respectively. It is assumed that velocity and thermal slip effects are present in the flow and a non-uniform magnetic field B is applied perpendicular to the plate. Under the above assumptions with viscous dissipation, Joule heating and thermal radiation, physical model and governing equations are given by;

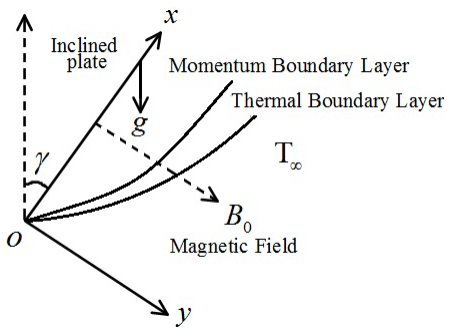

Figure 1 Geometry of the problem.

$$\frac{\partial u}{\partial x}+\frac{\partial v}{\partial y}=0, \tag{1}$$

$$u\frac{\partial u}{\partial x}+v\frac{\partial u}{\partial y}=\upsilon\frac{\partial^2 u}{\partial y^2}+g\beta\left(T-T_\infty\right)\cos\gamma-\frac{\sigma B^2}{\rho}\left(u-U_\infty\right)-\frac{\upsilon u}{K_p^*}, \tag{2}$$

$$\rho C_p\left(u\frac{\partial T}{\partial x}+v\frac{\partial T}{\partial y}\right)=\kappa\frac{\partial^2 T}{\partial y^2}+\mu\left(\frac{\partial u}{\partial y}\right)^2+\sigma B^2\left(u-U_\infty\right)^2+Q\left(T-T_\infty\right)-\frac{\partial q_r}{\partial y}, \tag{3}$$

where $u=u(x,y)$ is the velocity of the fluid along the x axis [*m/s*],

$v=v(x,y)$ is the velocity of the fluid along the y axis [*m/s*],

$T=T(x,y)$ is temperature of the fluid [*Kelvin*],

β is the coefficient of thermal expansion [*per Kelvin*],

g is the acceleration due to gravity [m/s^2],

$\upsilon=\mu/\rho$ is the kinematic viscosity [m^2/s],

μ is the coefficient of viscosity [Ns/m^2],

ρ is the fluid density [kg/m^3],

σ is fluid electrical conductivity [*Siemens/m*],

$B = B_0 / \sqrt{x}$ is the non-uniform magnetic field working normal to the plate [*weber/m*^{2}],

K_p^* is permeability coefficient of porous medium [*m*^{2}],

Q is the heat source/sink [*joule/(m*^{3} *s Kelvin)*],

C_p is the specific heat at constant pressure [*joule/(kg Kelvin)*],

κ is the thermal conductivity [*watts/ (m Kelvin)*],

q_r is the radiative heat flux [*watts/m*^{2}],

U_∞ is the free stream velocity [*m/s*],

T_∞ is the free stream temperature [*Kelvin*].

The boundary conditions are;

$$\left.\begin{aligned} &u = L\left(\frac{\partial u}{\partial y}\right), v = -V_w, T = T_w + K\left(\frac{\partial T}{\partial y}\right) \ at \ y = 0, \\ &u \to U_\infty, T \to T_\infty \ \ as \ \ y \to \infty, \end{aligned}\right\} \tag{4}$$

where K is the thermal slip factors [*m*] at $y = 0$,

L is the velocity slip factors [*m*] at $y = 0$,

V_w is the suction/injection velocity [*m/s*] at the plate,

T_w is the variable temperature [*Kelvin*] of the plate.

The radiative heat flux q_r , under Rosseland approximation has the form;

$$q_r = -\frac{4\sigma^*}{3k^*}\frac{\partial T^4}{\partial y}, \tag{5}$$

where k^* is the absorption coefficient [m^{-1}],

σ^* is the Stefan Boltzmann constant [*watts/ (m*^{2} *Kelvin*^{4}*)*].

By using truncated Taylor series about the free stream temperature, we have;

$$T^4 \cong 4T_\infty^3 T - 3T_\infty^4. \tag{6}$$

Method of solution

Introducing similarity transformation and non-dimensional parameters

$$\psi = \sqrt{U_\infty \upsilon x} f(\eta), \ \eta = y\sqrt{\frac{U_\infty}{\upsilon x}} \text{ and } \theta(\eta) = \frac{T - T_\infty}{T_w - T_\infty}, \tag{7}$$

such that $u = \frac{\partial \psi}{\partial y}$, $v = -\frac{\partial \psi}{\partial x}$ so that equation of continuity is identically satisfied, where η is the similarity variable and $f(\eta)$ is the similarity function. Using Eq. (7) into Eqs. (2) - (3), we get;

$$f''' - M^2(f' - 1) + \frac{1}{2}ff'' + \lambda\theta\cos\gamma - \frac{1}{K_p}f' = 0, \tag{8}$$

$$(1+R)\theta'' + Ec\,\mathrm{Pr}\left\{(f'')^2 + M^2(f'-1)^2\right\} + \mathrm{Pr}\left\{\frac{1}{2}f\theta' + f'\theta + \delta\theta\right\} = 0, \tag{9}$$

Corresponding boundary conditions are reduced to;

$$\left.\begin{array}{l} f = S,\ f' = S_v,\ \theta = 1 + S_T\theta' \ \ at\ \eta = 0, \\ f' \to 1 \text{ and } \theta \to 0 \ \ as\ \ \eta \to \infty, \end{array}\right\} \tag{10}$$

where differentiation with respect to η is denoted by prime and dimensionless parameters are;

$\lambda = \dfrac{g\beta^* T_0}{U_\infty^2}$ is mixed convection parameter,

$M^2 = \dfrac{\sigma B_0^2}{\rho U_\infty}$ is magnetic parameter,

$K_p = \dfrac{U_\infty K_p^*}{\upsilon x}$ is permeability parameter,

$Ec = \dfrac{U_\infty^2}{c_p\left(T_w - T_\infty\right)}$ is Eckert number,

$\mathrm{Pr} = \dfrac{\mu C_p}{\kappa}$ is Prandtl number,

$R = \dfrac{16\sigma^* T_\infty^3}{3\kappa k^*}$ is radiation parameter,

$\delta = \dfrac{Qx}{\rho c_p U_\infty}$ is heat source/sink parameter,

$S = 2\sqrt{\dfrac{x}{U_\infty \upsilon}}V_w$ is suction/injection parameter,

$S_T = K\sqrt{\dfrac{U_\infty}{\upsilon x}}$ is thermal slip parameter

$S_v = L\sqrt{\dfrac{U_\infty}{\upsilon x}}$ is velocity slip parameter.

Local skin friction coefficient and dimensionless rate of heat transfer at the plate are given by;

$$C_f = \frac{2\tau_w}{\rho u_e^2} = 2\,\mathrm{Re}_x^{-1/2} f''(0),\ Nu_x = \frac{xq_w}{k(T_w - T_\infty)} = -\mathrm{Re}_x^{1/2}\theta'(0), \tag{11}$$

where the heat flux q_w and the wall shear stress τ_w are given by;

$q_w = -k\left(\dfrac{\partial T}{\partial y}\right)_{y=0}$, $\tau_w = \mu\left(\dfrac{\partial u}{\partial y}\right)_{y=0}$ and $\mathrm{Re}_x = u_e(x)\dfrac{x}{\upsilon}$ is local Reynolds number.

Since Eqs. (8) - (9) are nonlinear coupled third and second order differential equations, respectively, whose closed form solution cannot be derived. Hence Eqs. (8) - (9) are solved numerically under boundary conditions (10) using Runge-Kutta fourth order method with shooting technique. According to the Runge-Kutta fourth order method, to obtain the solution a system of first order differential equations is constructed from Eqs. (8) - (9) as follows;

$$f_1' = f_2,$$
$$f_2' = f_3,$$
$$f_3' = M^2\left(f_2 - 1\right) - \frac{1}{2} f_1 f_3 - \lambda f_4 \cos\gamma + \frac{1}{K_p} f_2,$$
$$f_4' = f_5,$$
$$f_5' = -\frac{\Pr}{\left(1+R\right)}\left\{ Ec\left\{\left(f_3\right)^2 + M^2\left(f_2 - 1\right)^2\right\} + \left\{\frac{1}{2} f_1 f_5 + f_2 f_4 + \delta f_4\right\}\right\},$$

where $f_1 = f, f_2 = f', f_3 = f'', f_4 = \theta, f_5 = \theta'$.

Initial conditions are;

$$f_1\left(0\right) = S,\ f_2\left(0\right) = S_v,\ f_3\left(0\right) = s_1,\ f_4\left(0\right) = 1 + S_T s_2,\ f_5\left(0\right) = s_2.$$

In order to get a solution step by step integration is carried out. To start the integration, values of f_1, f_2, f_3, f_4, f_5 are required at $\eta = 0$ but from the conditions given in (10), it is clear that values of f_3 and f_5 are not known. According to the shooting technique values are assumed to be s_1 and s_2 and accuracy of the assumed values of s_1 and s_2 are checked by comparing the calculated values of different variables at the terminal point i.e. $\eta_\infty = 8$ with the given values. The procedure is repeated until the results up to the accuracy 10^{-5} are obtained. The results are carried out using MATLAB.

Results and discussion

In this section, effects of various physical parameters on fluid properties are presented through figures and table. From **Figures 4 - 18**, solid and dotted curves have been drawn for heat sink $\left(\delta = -0.5\right)$ and heat source $\left(\delta = 0.5\right)$, respectively.

Figures 2 and **3** show that fluid velocity and temperature increase with increasing heat source parameter. By increasing the heat source parameter we supply some amount of energy/heat to the fluid and this supply cause jump in fluid velocity and temperature. The increasing velocity and temperature results in more skin friction and a lesser rate of heat transfer respectively, which is consistent with the data given in **Table 1**.

It is observed from **Figures 4** and **5** that fluid velocity and temperature increase with increasing Eckert number for both heat source and heat sink. This is because the greater Eckert number corresponds with more dissipative heat. This increasing velocity causes more skin friction. Due to the increasing temperature of the fluid, the temperature difference decreases, and this results in decreasing Nusselt number, as seen from **Table 1**.

The effect of angle of inclination on fluid velocity and temperature is shown in **Figures 6** and **7**. As the angle of inclination increases, the velocity of the fluid decreases while the temperature increases. Because of this decreasing fluid velocity, there will be lesser skin friction.

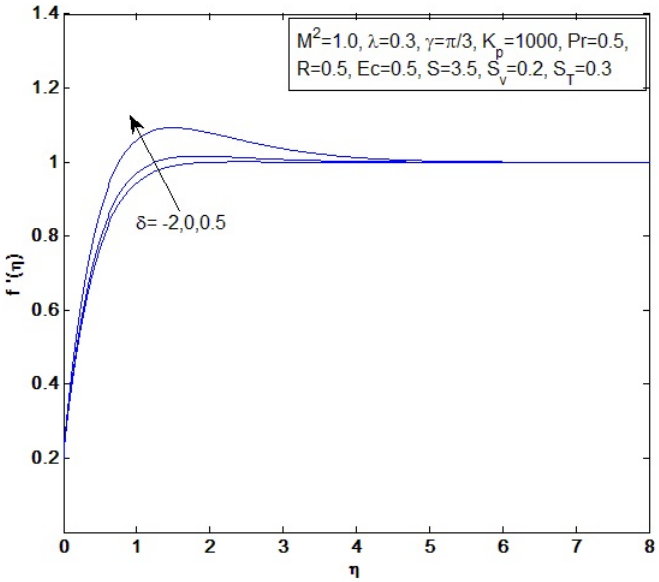

Figure 2 Velocity profiles versus η for different values of δ .

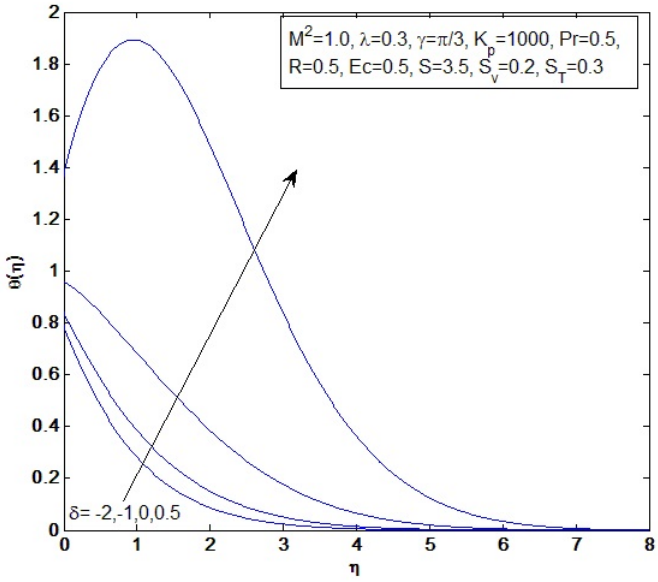

Figure 3 Temperature profiles versus η for different values of δ .

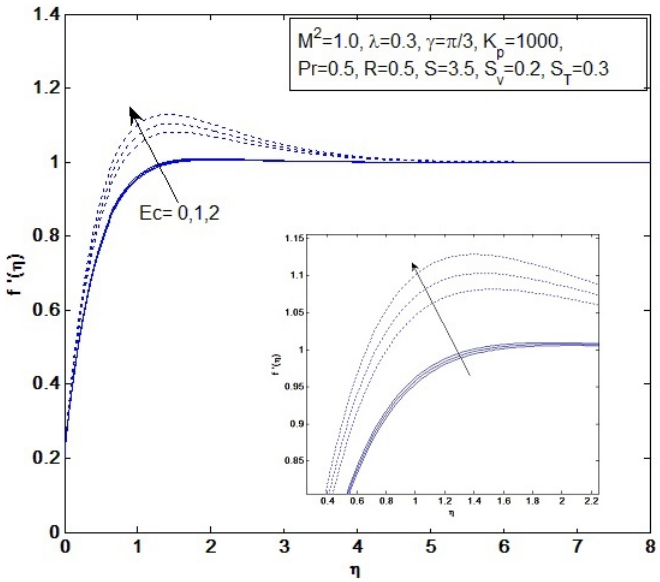

Figure 4 Velocity profiles versus η for different values of Ec .

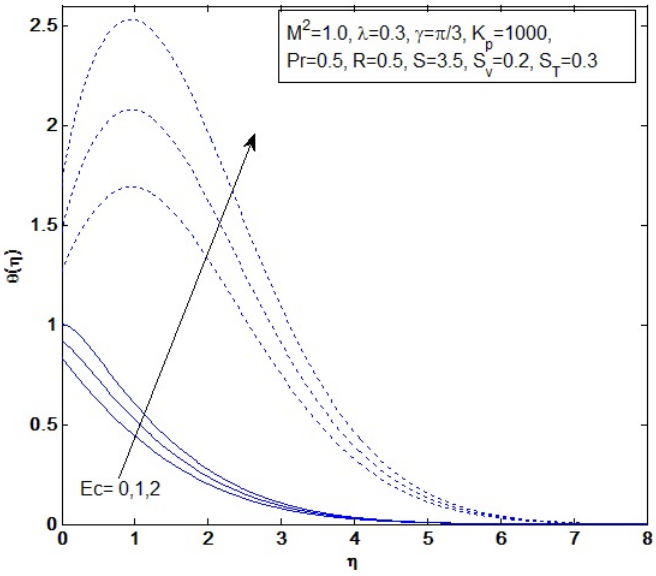

Figure 5 Temperature profiles versus η for different values of Ec .

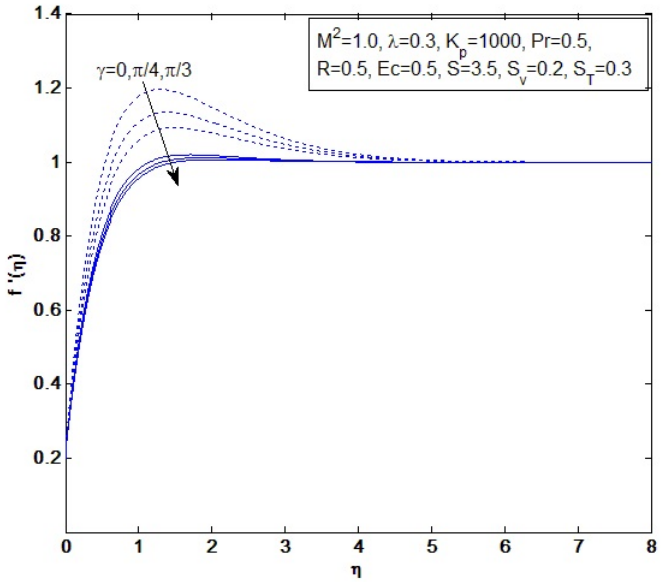

Figure 6 Velocity profiles versus η for different values of γ.

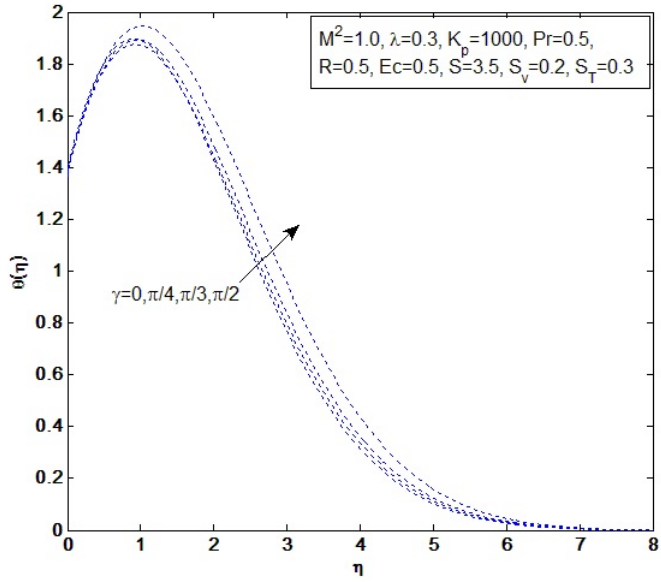

Figure 7 Temperature profiles versus η for different values of γ.

Figure 8 depicts the dual nature of magnetic parameter on the fluid velocity with heat source and heat sink. With increasing magnetic parameter there is an enhancement in fluid velocity for heat sink while the opposite impact has been noticed for heat source. The effect of magnetic parameter on fluid temperature is presented through **Figure 9**. The figure shows that fluid temperature increases with increasing magnetic parameter.

It is noticed from **Figures 10** and **11** that both fluid velocity and temperature decrease with increasing Prandtl number for both heat source and sink. When Prandtl number increases, kinematic viscosity dominates the thermal diffusivity and as a result, there is a drop in fluid velocity and temperature. This drop in fluid velocity causes lesser skin friction while the drop in temperature results in increasing temperature difference and due to this increasing temperature difference rate of heat transfer increases, as observed from **Table 1**.

Fluid velocity and temperature increase with increasing radiation parameter for both heat source and sink as noted from **Figures 12** and **13**. The reason behind this is the fluid particles consume the radiated heat and get energized. Due to this increasing fluid velocity skin friction increases and increasing temperature decreases the temperature difference and results in decreasing Nusselt number, as can be seen from **Table 1**.

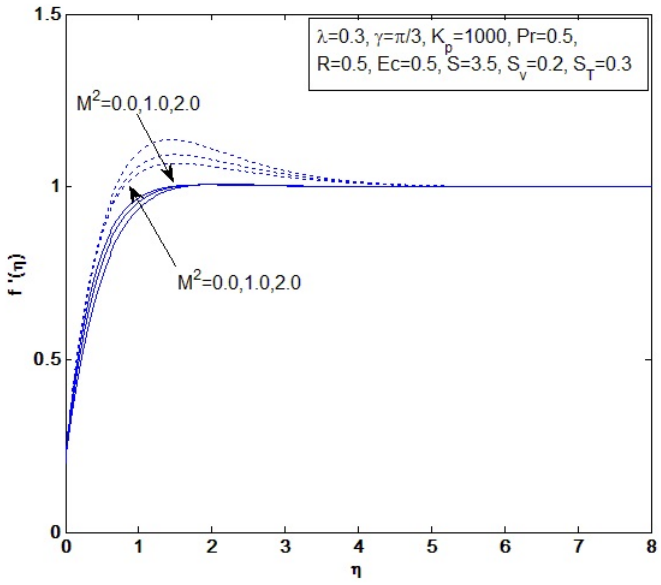

Figure 8 Velocity profiles versus η for different values of M^2.

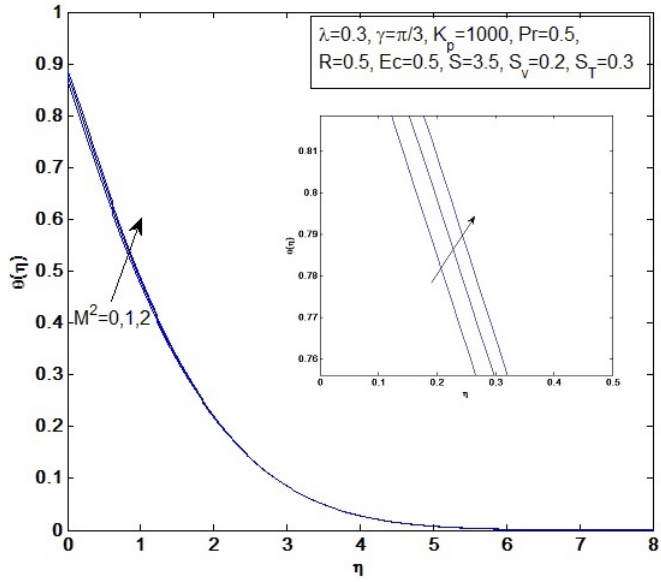

Figure 9 Temperature profiles versus η for different values of M^2.

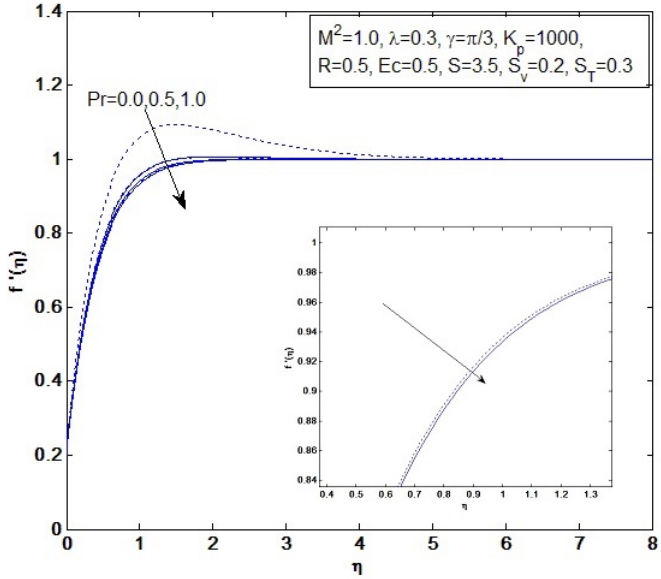

Figure 10 Velocity profiles versus η for different values of Pr .

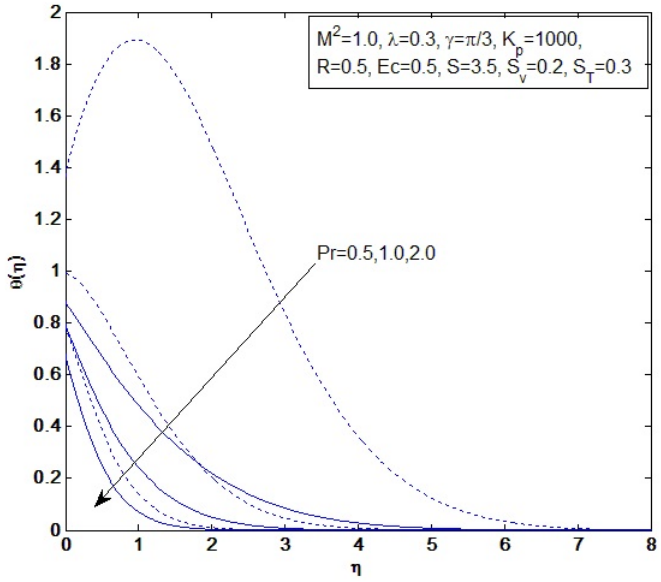

Figure 11 Temperature profiles versus η for different values of Pr .

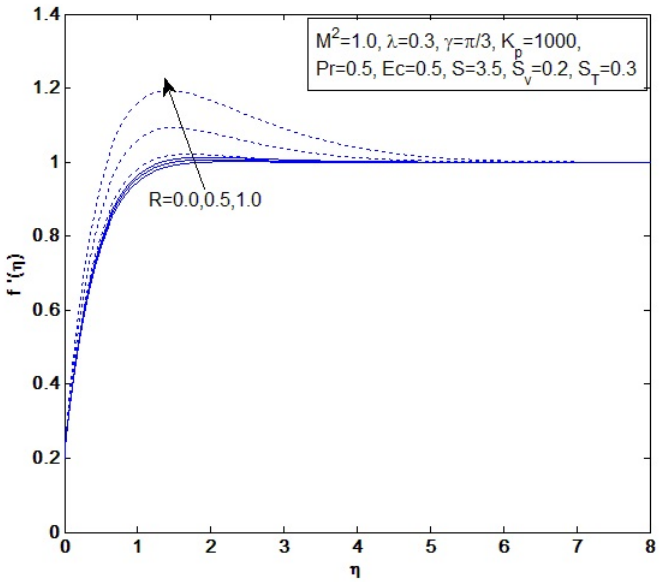

Figure 12 Velocity profiles versus η for different values of R .

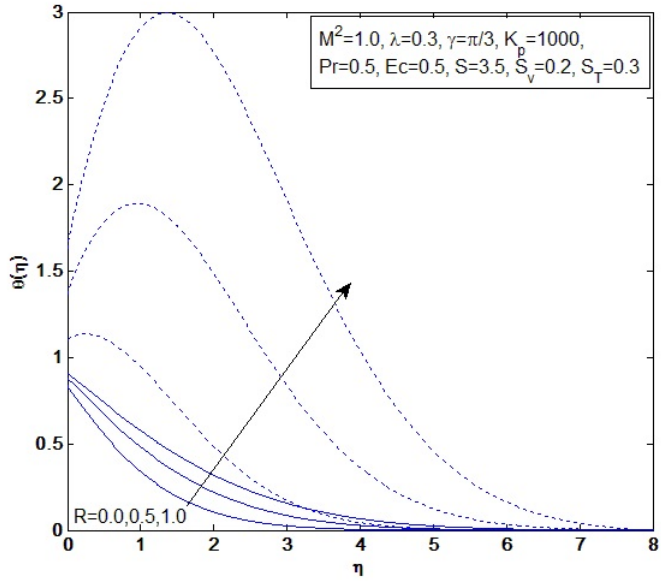

Figure 13 Temperature profiles versus η for different values of R .

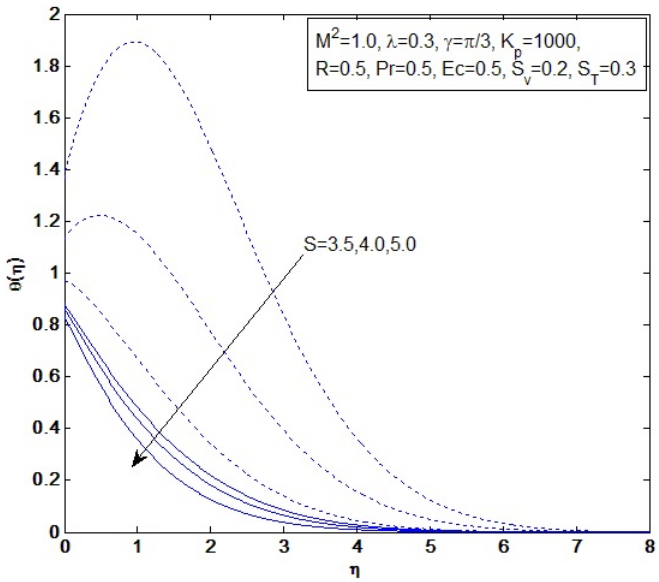

Figure 14 Temperature profiles versus η for different values of S .

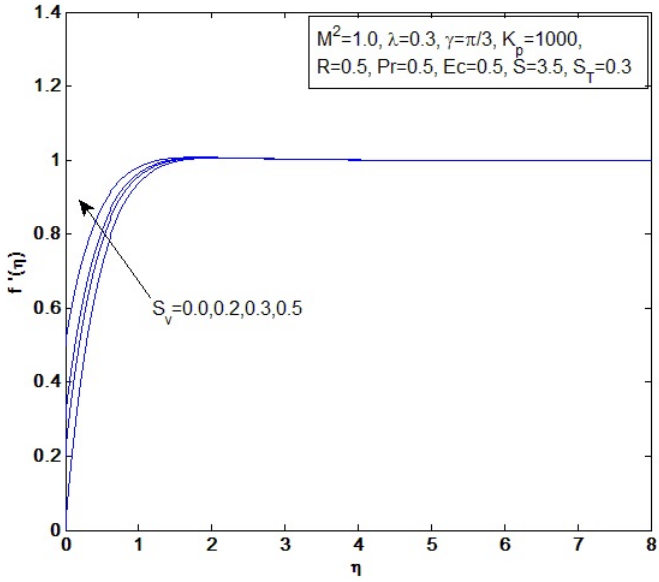

Figure 15 Velocity profiles versus η for different values of S_V .

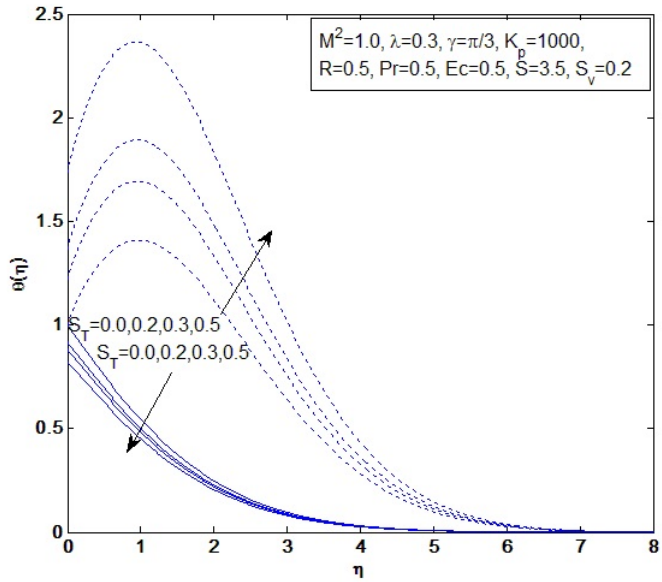

Figure 16 Temperature profiles versus η for different values of S_T.

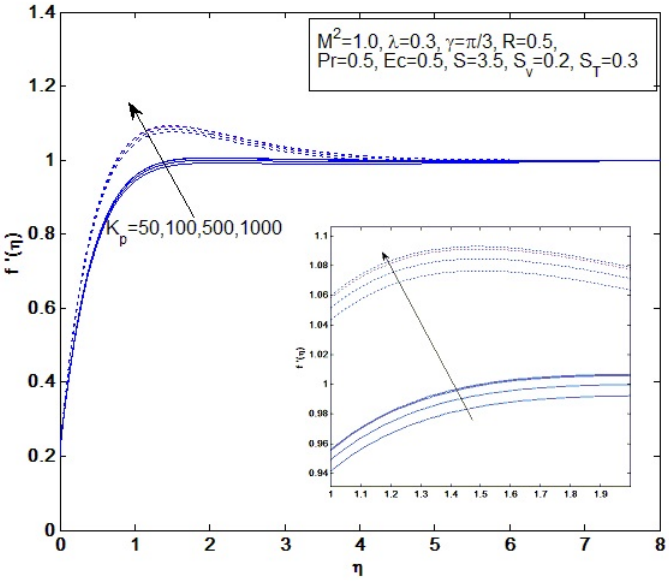

Figure 17 Velocity profiles versus η for different values of K_p.

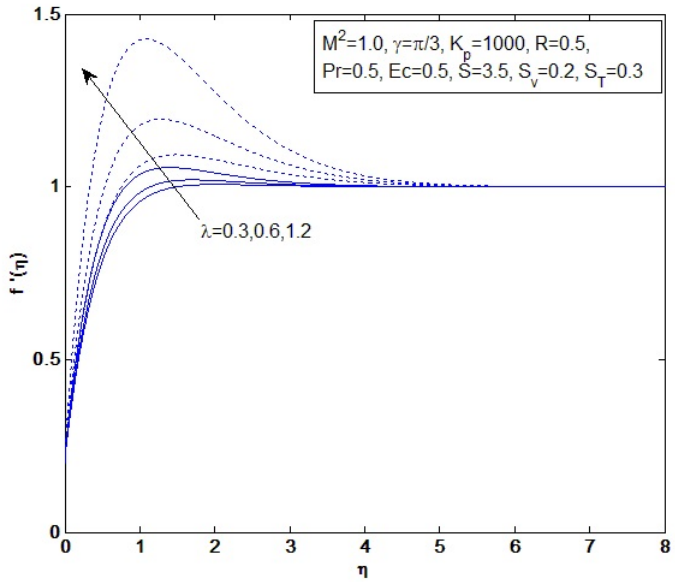

Figure 18 Velocity profiles versus η for different values of λ .

It is noted from **Figure 14** that fluid temperature decreases with increasing suction parameter. When suction parameter is increased more amount of fluid is sucked by the wall and as a result temperature of the fluid decreases and Nusselt number increases.

Figure 15 shows that fluid velocity increases with increasing velocity slip parameter. Although the fluid velocity increases with increasing velocity slip parameter, but due to slip effect skin friction coefficient decreases.

Figure 16 demonstrates that fluid temperature increases with increasing thermal slip parameter for heat source while there is reverse effect of the parameter for heat sink. When thermal slip parameter enhances in the presence of heat source there will be a sudden jump in the temperature of fluid particles in the layer adjacent to the plate while there will be a sudden drop in the temperature of fluid particles in the layer adjacent for heat sink.

Table 1 Numerical values of skin friction coefficient and Nusselt number at the surface of the plate for various values of physical parameters.

M^2	λ	γ	K_p	R	Pr	Ec	δ	S	S_v	S_T	$f''(0)$	$-\theta'(0)$
0.0	0.3	$\pi/3$	1000	0.5	0.5	0.5	0.5	3.5	0.2	0.3	1.777	−1.015
2.0	0.3	$\pi/3$	1000	0.5	0.5	0.5	0.5	3.5	0.2	0.3	1.885773	−1.015
0.0	0.3	$\pi/3$	1000	0.5	0.5	0.5	−0.5	3.5	0.2	0.3	1.48487	0.4441
2.0	0.3	$\pi/3$	1000	0.5	0.5	0.5	−0.5	3.5	0.2	0.3	1.77264	0.413
1.0	**0.3**	$\pi/3$	1000	0.5	0.5	0.5	0.5	3.5	0.2	0.3	1.81718	−1.015
1.0	**1.2**	$\pi/3$	1000	0.5	0.5	0.5	0.5	3.5	0.2	0.3	2.4981	−1.131
1.0	**0.3**	$\pi/3$	1000	0.5	0.5	0.5	−0.5	3.5	0.2	0.3	1.64837	0.4258
1.0	**1.2**	$\pi/3$	1000	0.5	0.5	0.5	−0.5	3.5	0.2	0.3	1.87866	0.402
1.0	0.3	$\pi/4$	1000	0.5	0.5	0.5	0.5	3.5	0.2	0.3	1.91224	−1.010
1.0	0.3	$\pi/2$	1000	0.5	0.5	0.5	0.5	3.5	0.2	0.3	1.57181	−1.078
1.0	0.3	$\pi/4$	1000	0.5	0.5	0.5	−0.5	3.5	0.2	0.3	1.68027	0.422

M^2	λ	γ	K_p	R	Pr	Ec	δ	S	S_v	S_T	$f''(0)$	$-\theta'(0)$
1.0	0.3	$\pi/2$	1000	0.5	0.5	0.5	−0.5	3.5	0.2	0.3	1.57205	0.437
1.0	0.3	$\pi/3$	**100**	0.5	0.5	0.5	0.5	3.5	0.2	0.3	1.80572	−1.015
1.0	0.3	$\pi/3$	**1000**	0.5	0.5	0.5	0.5	3.5	0.2	0.3	1.81718	−1.015
1.0	0.3	$\pi/3$	**100**	0.5	0.5	0.5	−0.5	3.5	0.2	0.3	1.63688	0.42766
1.0	0.3	$\pi/3$	**1000**	0.5	0.5	0.5	−0.5	3.5	0.2	0.3	1.64837	0.4258
1.0	0.3	$\pi/3$	1000	**0.5**	0.5	0.5	0.5	3.5	0.2	0.3	1.81718	−1.015
1.0	0.3	$\pi/3$	1000	**2.0**	0.5	0.5	0.5	3.5	0.2	0.3	2.529445	−4.75370
1.0	0.3	$\pi/3$	1000	**0.5**	0.5	0.5	−0.5	3.5	0.2	0.3	1.64837	0.4258
1.0	0.3	$\pi/3$	1000	**2.0**	0.5	0.5	−0.5	3.5	0.2	0.3	1.68187	0.233
1.0	0.3	$\pi/3$	1000	0.5	**0.5**	0.5	0.5	3.5	0.2	0.3	1.81718	−1.015
1.0	0.3	$\pi/3$	1000	0.5	**2.0**	0.5	0.5	3.5	0.2	0.3	1.60946	0.8
1.0	0.3	$\pi/3$	1000	0.5	**0.5**	0.5	−0.5	3.5	0.2	0.3	1.64837	0.4258
1.0	0.3	$\pi/3$	1000	0.5	**2.0**	0.5	−0.5	3.5	0.2	0.3	1.59718	1.155
1.0	0.3	$\pi/3$	1000	0.5	0.5	**0.2**	0.5	3.5	0.2	0.3	1.80753	−0.89
1.0	0.3	$\pi/3$	1000	0.5	0.5	**0.5**	0.5	3.5	0.2	0.3	1.81718	−1.015
1.0	0.3	$\pi/3$	1000	0.5	0.5	**0.2**	−0.5	3.5	0.2	0.3	1.64599	0.482
1.0	0.3	$\pi/3$	1000	0.5	0.5	**0.5**	−0.5	3.5	0.2	0.3	1.64837	0.4258
1.0	0.3	$\pi/3$	1000	0.5	0.5	0.5	**−2.0**	3.5	0.2	0.3	1.6234	0.7286
1.0	0.3	$\pi/3$	1000	0.5	0.5	0.5	**−1.0**	3.5	0.2	0.3	1.63627	0.5605
1.0	0.3	$\pi/3$	1000	0.5	0.5	0.5	**0.0**	3.5	0.2	0.3	1.6744	0.1769
1.0	0.3	$\pi/3$	1000	0.5	0.5	0.5	**0.5**	3.5	0.2	0.3	1.81718	−1.015
1.0	0.3	$\pi/3$	1000	0.5	0.5	0.5	0.5	**3.5**	0.2	0.3	1.81718	−1.015
1.0	0.3	$\pi/3$	1000	0.5	0.5	0.5	0.5	**5.0**	0.2	0.3	1.9474	0.16
1.0	0.3	$\pi/3$	1000	0.5	0.5	0.5	−0.5	**3.5**	0.2	0.3	1.64837	0.4258
1.0	0.3	$\pi/3$	1000	0.5	0.5	0.5	−0.5	**5.0**	0.2	0.3	1.90825	0.592
1.0	0.3	$\pi/3$	1000	0.5	0.5	0.5	0.5	3.5	**0.2**	0.3	1.81718	−1.015
1.0	0.3	$\pi/3$	1000	0.5	0.5	0.5	0.5	3.5	**0.5**	0.3	1.219521	−0.8
1.0	0.3	$\pi/3$	1000	0.5	0.5	0.5	−0.5	3.5	**0.2**	0.3	1.64837	0.4258
1.0	0.3	$\pi/3$	1000	0.5	0.5	0.5	−0.5	3.5	**0.5**	0.3	1.1214	0.4686
1.0	0.3	$\pi/3$	1000	0.5	0.5	0.5	0.5	3.5	0.2	**0.2**	1.79783	−0.950
1.0	0.3	$\pi/3$	1000	0.5	0.5	0.5	0.5	3.5	0.2	**0.5**	1.86983	−1.210
1.0	0.3	$\pi/3$	1000	0.5	0.5	0.5	−0.5	3.5	0.2	**0.2**	1.65176	0.448
1.0	0.3	$\pi/3$	1000	0.5	0.5	0.5	−0.5	3.5	0.2	**0.5**	1.64279	0.38615

It is noticed from **Figures 17** and **18** that fluid velocity increases with increasing permeability parameter or mixed convection parameter. For larger permeability parameter there will be more assistance to the fluid to flow through the porous medium and as a result velocity increases. Increasing mixed convection parameter will increase buoyancy force and due to this velocity of the fluid increases. Because of increasing velocity, skin friction coefficient increase which is consistent with the data given in **Table 1**.

Conclusions

The combined effect of radiation and viscous dissipation on MHD mixed convective flow along a porous plate inclined with angle γ from the vertical in porous medium is investigated. In view of the above results, the following conclusions have been made:

1) In order to enhance the fluid velocity with low temperature, angle of inclination from the vertical i.e. γ must be less.

2) Larger mixed convection parameter, Eckert number, permeability parameter or radiation parameter enhances the fluid velocity.

3) To achieve the objective of reducing fluid temperature, Eckert number, heat source/sink parameter or radiation parameter must be reduced while thermal slip parameter in the presence of heat sink must be enlarged.

4) Skin friction coefficient decreases for decreasing values of radiation parameter, Eckert number, mixed convection parameter or permeability parameter.

5) To enhance the dimensionless rate of heat transfer, Eckert number or radiation parameter must be decreased and Prandtl number must be increased.

Acknowledgements

The authors would like to thank the Editor and anonymous reviewers for their careful reading and constructive comments and suggestions, which helped a lot in the improvement of the manuscript.

References

[1] VCA Ferraro and C Plumpton. *An introduction to magneto-fluid mechanics*. Clarendon Press, Oxford, 1966, p. 191-6.

[2] Y Jaluria. *Natural convection heat and mass transfer*. Vol I. Pergamon Press, Oxford, 1980, p. 152-60.

[3] N Afzal and T Hussain. Mixed convection over a horizontal plate. *ASME J. Heat Tran.* 1984; **106**, 240.

[4] MA Hossain and HS Takhar. Radiation effect on mixed convection along a vertical plate withuniform surface temperature. *Heat Mass Tran*. 1996; **31**, 243-8.

[5] I Pop and DB Ingham. *Convective heat transfer: Mathematical and computational modelling of viscous fluids and porous media*. 1st ed. Pergamon, Amsterdam, Netherlands, 2001, p. 125-32.

[6] RA Damesh. Magnetohydrodynamics-mixed convection from radiate vertical isothermal surface embedded in a saturated porous media. *J. Appl. Mech.* 2006; **73**, 54-9.

[7] O Aydin and A Kaya. Mixed convection of a viscous dissipating fluid about a vertical flat plate. *Appl. Math. Model*. 2007; **31**, 843-53.

[8] K Cao and J Baker. Slip effects on mixed convective flow and heat transfer from a vertical plate. *Int. J. Heat Mass Tran.* 2009; **52**, 3829-41.

[9] K Bhattacharyya, S Mukhopadhyay and GC Layek. MHD boundary layer slip flow and heat transfer over a flat plate. *Chin. Phys. Lett.* 2011; **28**, 024701.

[10] MM Nandeppanavar, K Vajravelu and MS Abel. Heat transfer in MHD viscoelastic boundary layer flow over a stretching sheet with thermal radiation and non-uniform heat source/sink. *Commun. Nonlinear Sci. Numer. Simulat*. 2011; **16**, 3578-90.

[11] MM Rashidi, B Rostami, N Freidoonimehr and S Abbasbandy. Free convective heat and mass transfer for MHD fluid flow over a permeable vertical stretching sheet in the presence of the radiation and buoyancy effects. *Ain Shams Eng. J*. 2014; **5**, 901-12.

[12] PR Sharma and S Choudhary. Radiation and chemical reaction effects on unsteady slip flow over a semi-infinite vertical porous plate embedded in a porous medium in the presence of inclined magnetic field. *Int. J. Latest Tech. Eng. Manag. Appl. Sci*. 2014; **3**, 17-24.

[13] S Das, RN Jana and OD Makinde. Magnetohydrodynamic mixed convective slip flow over an inclined porous plate with viscous dissipation and Joule heating. *Alexandria Eng. J.* 2015; **54**, 251-61.

[14] AK Pandey and M Kumar. Effect of viscous dissipation and suction/injection on MHD nanofluid flow over a wedge with porous medium and slip. *Alexandria Eng. J*. 2016; **55**, 3115-23.

[15] PR Sharma, S Sinha, RS Yadav and Anatoly N Filippov. MHD mixed convective stagnation point flow along a vertical stretching sheet with heat source/sink. *Int. J. Heat Mass Tran*. 2018; **117**, 780-6.
[16] MV Krishna, NA Ahamad and AJ Chamkha. Hall and ion slip effects on unsteady MHD free convective rotating flow through a saturated porous medium over an exponential accelerated plate. *Alexandria Eng. J*. 2020; **59**, 565-77.
[17] M Sheikholeslami, SA Farshad and Z Said. Analyzing entropy and thermal behavior of nanomaterial through solar collector involving new tapes. *Int. Comm. Heat Mass Tran.* 2021; **123,** 105190.
[18] M Sheikholeslami, SA Farshad, Z Ebrahimpour and Z Said. Recent progress on flat plate solar collectors and photovoltaic systems in the presence of nanofluid: A review. *J. Cleaner Prod*. 2021; **293**, 126119.
[19] M Sheikholeslami and SA Farshad. Investigation of solar collector system with turbulator considering hybrid nanoparticles. *Renew. Energ*. 2021; **171**, 1128-58.